Possibilistic Uncertainty Modeling with Hyperellipsoids

Julian Behrend, Tom Könecke, Mario Rosenfelder, Jan Schneider,
Michael Hanss, and Peter Eberhard
*Institute of Engineering and Computational Mechanics, University of Stuttgart,
Pfaffenwaldring 9, 70569 Stuttgart, Germany*

Abstract. The quantification of sparse, imprecise knowledge using possibility theory traditionally forces a compromise between computational efficiency and geometric accuracy. Standard interval arithmetic over axis-aligned hyperrectangles ignores parameter dependencies and yields overly conservative bounds, while sampling-based techniques capture these dependencies but remain computationally intensive and fail to deliver guarantees. By leveraging geometric properties of ellipsoids, we address these challenges by providing a comprehensive operational calculus for possibilistic uncertainty representation using hyperellipsoids. This framework provides methodologies to construct ellipsoidal possibility distributions from data, fuse multiple knowledge sources, propagate distributions analytically through affine functions, and extract both marginal and joint distributions. Furthermore, we demonstrate the practical efficacy of these ellipsoidal possibility distributions by applying them to a filtering application for a mobile robot localization problem.

Keywords: uncertainty quantification, fuzzy arithmetic, possibility theory, imprecise probabilities, robot localization, dynamic state estimation, ellipsoidal calculus

1. Introduction

In the analysis of complex engineering systems, possibility theory provides a rigorous mathematical framework for handling both epistemic and aleatory uncertainty by bounding sets of consistent probability measures. However, the numerical implementation of possibilistic models has encountered structural and computational trade-offs. Traditional interval arithmetic relies on axis-aligned hyperrectangles. Recent approaches have favored sampling-based techniques to address parameter identification under uncertainty (Könecke et al., 2025), advanced sampling techniques for possibilistic forward propagation (Mäck and Hanss, 2021) and a particle-based formulation of possibilistic filters (Hose and Hanss, 2021). While being effective at mapping nonlinearities, sampling methods suffer from the curse of dimensionality and fail to provide trustworthy certainty guarantees.

To resolve these limitations, this paper proposes the use of hyperellipsoids as the foundational geometric structure for possibilistic uncertainty representation. Rather than relying on discrete point clouds or intervals, we want to utilize well-studied, analytically tractable properties of hyperellipsoids to allow handling multi-variate possibility distributions. While one can derive an ellipsoidal possibility distribution leveraging given expert knowledge (Kreinovich et al., 2007), this work focuses on the construction of an ellipsoidal possibility distribution from data or a probability density function. In the domain of statistical inference, Martin (2025) uses ellipsoids for the efficient construction of possibility distributions from data, while Martin and Williams (2025) further propose ellipsoid-based Gaussian possibility distributions. As ellipsoids naturally arise in Gaussian distributions, they also appear together in possibilistic filtering approaches like for the Kalman filter (Ferrero et al., 2021), (Matía et al., 2021).

This paper novelly establishes a comprehensive operational calculus for possibilistic uncertainty quantification based on ellipsoidal representations. The proposed approach includes the construction of ellipsoidal possibility distributions, their fusion, and their analytical propagation. We also provide details on how to perform marginalization and compute joint distributions within this ellipsoidal setting. In addition to the theoretical development, these contributions are integrated into a recursive possibilistic filter for dynamic state estimation of a real-world mobile robot, demonstrating the practical relevance of the framework for safety-critical robotic applications.

The remainder of this paper is structured as follows. Section 2 establishes the theoretical background of possibility theory and ellipsoidal calculus. Section 3 introduces the ellipsoidal possibility distributions and details the methodologies for their construction, fusion, propagation, and marginalization, as well as the formation of joint distributions. Finally, Section 4 presents an example of a possibilistic filtering procedure in dynamic state estimation for a mobile robot to demonstrate the practical application of this framework.

2. Background

2.1. Possibility Theory

Possibility theory provides a framework for handling epistemic and aleatory uncertainty by describing the possible values of an imprecise variable $\boldsymbol{X}$ that is a measurable function $\boldsymbol{X} : \Omega \to \mathcal{V}$ from a sample space Ω to a value space $\mathcal{V}$, in this case $\mathbb{R}^n$.

The basic building block of possibility theory is the possibility distribution $\pi_{\boldsymbol{X}} : \Omega \to [0, 1]$. The function $\pi_{\boldsymbol{X}}(\boldsymbol{x})$ returns the degree of possibility that $\boldsymbol{X}$ takes the value $\boldsymbol{x}$, ranging from 0 (impossible) to 1 (fully possible). A possibility distribution is normal if $\sup_{\boldsymbol{x}} \pi_{\boldsymbol{X}}(\boldsymbol{x}) = 1$, and subnormal if $\sup_{\boldsymbol{x}} \pi_{\boldsymbol{X}}(\boldsymbol{x}) < 1$. The information contained in $\pi_{\boldsymbol{X}}$ is equivalently represented by a family of nested α-cuts $\mathcal{C}_\pi^\alpha = \{\boldsymbol{x} \in \mathbb{R}^n \mid \pi_{\boldsymbol{X}}(\boldsymbol{x}) \geq \alpha\}$ for any $\alpha \in [0, 1]$. For any two levels α_1 and α_2, with $0 \leq \alpha_1 \leq \alpha_2 \leq 1$, the inclusion $\mathcal{C}_\pi^{\alpha_2} \subseteq \mathcal{C}_\pi^{\alpha_1}$ holds. This nesting property is a fundamental characteristic of possibilistic representations.

A normal possibility distribution induces for an event $E \subseteq \Omega$ both the possibility measure

$$\Pi_{\boldsymbol{X}}(E) = \sup_{\boldsymbol{x} \in E} \pi_{\boldsymbol{X}}(\boldsymbol{x}) \tag{1}$$

and the necessity measure

$$\mathrm{N}_{\boldsymbol{X}}(E) = 1 - \Pi_{\boldsymbol{X}}(\Omega \setminus E) = 1 - \sup_{\boldsymbol{x} \notin E} \pi_{\boldsymbol{X}}(\boldsymbol{x}) \, . \tag{2}$$

By the definition of these dual measures, possibility theory serves as a framework for imprecise probabilities through the principle of consistency. A probability measure $\mathrm{P}_{\boldsymbol{X}}$ is *consistent* with $\pi_{\boldsymbol{X}}$ if

$$\mathrm{N}_{\boldsymbol{X}}(E) \leq \mathrm{P}_{\boldsymbol{X}}(E) \leq \Pi_{\boldsymbol{X}}(E) \qquad \forall E \subseteq \Omega \tag{3}$$

holds. Consequently, the α-cuts of a possibility distribution constitute sets with a guaranteed lower probability bound

$$\mathrm{P}(\mathcal{C}_\pi^\alpha) \geq 1-\alpha \qquad \forall \alpha \in [0,1] \; . \tag{4}$$

The possibility distribution is the elementary building block of possibility theory, defining both an upper and lower probability bound. In this elementary role, it is akin to the probability density function in probability theory, but notably diverges by following a non-additive framework, i.e., by requiring the supremum and infimum in its mathematical treatment in place of the sum or integral. This will be further elaborated in the following paragraphs.

In multivariate settings, where $\boldsymbol{X} = [\boldsymbol{X}_1, \dots, \boldsymbol{X}_q]$, the marginal distribution for a subset of q variables is obtained by projecting the joint distribution $\pi_{\boldsymbol{X}}$ onto the respective subspace

$$\pi_{\boldsymbol{X}_1}(\boldsymbol{x}_1) = \sup_{\boldsymbol{x}_2,\dots,\boldsymbol{x}_q} \pi_{\boldsymbol{X}}(\boldsymbol{x}_1, \dots, \boldsymbol{x}_q) \; . \tag{5}$$

Conversely, constructing a joint possibility distribution $\pi_{\boldsymbol{X}}(\boldsymbol{x}_1, \dots, \boldsymbol{x}_q) = \mathcal{J}(\pi_{\boldsymbol{X}_1}(\boldsymbol{x}_1), \dots, \pi_{\boldsymbol{X}_q}(\boldsymbol{x}_q))$ from marginal variables $\boldsymbol{X}_i$ requires modeling the dependencies using a copula $\mathcal{J} : [0,1]^q \to [0,1]$. For stochastically independent imprecise variables, the most specific consistency-preserving joint representation is given by

$$\pi_{\text{joint}}(\boldsymbol{x}_1, \dots, \boldsymbol{x}_q) = 1 - \left(1 - \min_{\boldsymbol{x}_1,\dots,\boldsymbol{x}_q} (\pi_{\boldsymbol{X}_1}(\boldsymbol{x}_1), \dots, \pi_{\boldsymbol{X}_q}(\boldsymbol{x}_q))\right)^q \; . \tag{6}$$

Proofs for this statement as well as further discussions on copulas can be found in (Hose, 2022).

Possibilistic propagation through a mapping $\boldsymbol{Y} = f(\boldsymbol{X})$ is governed by Zadeh's extension principle (Zadeh, 1975)

$$\pi_{\boldsymbol{Y}}(\boldsymbol{y}) = \sup_{\boldsymbol{x} \,|\, \boldsymbol{y}=f(\boldsymbol{x})} \pi_{\boldsymbol{X}}(\boldsymbol{x}) \; . \tag{7}$$

The extension principle ensures that the output distribution remains the most specific description consistent with the input uncertainty and the propagation model.

2.2. Ellipsoidal Calculus

A hyperellipsoid $\mathcal{E} \subset \mathbb{R}^n$, subsequently referred to as ellipsoid for simplicity, is defined as the set of points satisfying the quadratic inequality

$$\mathcal{E}(\boldsymbol{c}, \boldsymbol{P}) = \{\boldsymbol{x} \in \mathbb{R}^n \mid Q(\boldsymbol{x}, \boldsymbol{c}, \boldsymbol{P}) \leq 1\} \; , \qquad Q(\boldsymbol{x}, \boldsymbol{c}, \boldsymbol{P}) = (\boldsymbol{x} - \boldsymbol{c})^\mathsf{T} \boldsymbol{P} (\boldsymbol{x} - \boldsymbol{c}) \; , \tag{8}$$

parameterized by a center $\boldsymbol{c} \in \mathbb{R}^n$ and a symmetric positive-definite shape matrix $\boldsymbol{P} \in \mathbb{R}^{n \times n}$. The volume of $\mathcal{E}(\boldsymbol{c}, \boldsymbol{P})$ is proportional to $\det(\boldsymbol{P})^{-1/2}$. Degenerate ellipsoids also fall within this formulation with $\boldsymbol{P}$ being positive semi-definite. Such sets represent unbounded regions, e.g., cylinders or strips ($\operatorname{rank}(\boldsymbol{P}) < n$), with infinite volume.

Ellipsoidal sets can be inferred from data, for example, using the minimum volume enclosing ellipsoid (MVEE), which minimizes volume while enclosing all points and is efficiently solvable via Khachiyan's algorithm (Moshtagh, 2005).

The *intersection* of two ellipsoids is generally not an ellipsoid. For two ellipsoids $\mathcal{E}_1, \mathcal{E}_2$ with a non-empty intersection, a parameterized family of intersection-enclosing ellipsoids $\mathcal{E}_\lambda(\boldsymbol{c}_\lambda, \boldsymbol{P}_\lambda)$ can be defined by the convex combination $Q_\lambda = \lambda\, Q_1 + (1-\lambda)\, Q_2$ of their quadratic forms Q_1 and Q_2, where $\lambda \in [0,1]$. These ellipsoids guarantee the inclusion property $(\mathcal{E}_1 \cap \mathcal{E}_2) \subseteq \mathcal{E}_\lambda \subseteq (\mathcal{E}_1 \cup \mathcal{E}_2)$. This λ-ellipsoid approach yields an analytic expression for the parameters $\boldsymbol{c}_\lambda$ and $\boldsymbol{P}_\lambda$ and also applies to the intersection of degenerate and regular ellipsoids. For proofs and derivations see (Ros et al., 2002).

The *affine propagation* of an ellipsoid describes the process of determining the resulting ellipsoid for a variable $\boldsymbol{y} \in \mathbb{R}^m$ that is affinely related to another variable $\boldsymbol{x} \in \mathbb{R}^n$ whose domain is bounded by an ellipsoid $\mathcal{E}_{\boldsymbol{x}}(\boldsymbol{c}_{\boldsymbol{x}}, \boldsymbol{P}_{\boldsymbol{x}})$. The general form of such a relation is given by $\boldsymbol{A}\boldsymbol{x} + \boldsymbol{C}\boldsymbol{y} + \boldsymbol{b} = \boldsymbol{0}$, where $\boldsymbol{A} \in \mathbb{R}^{r\times n}$, $\boldsymbol{C} \in \mathbb{R}^{r\times m}$, and $\boldsymbol{b} \in \mathbb{R}^r$. The set of all possible values for $\boldsymbol{y}$ will also be an ellipsoid, provided that $\boldsymbol{A}$ and $\boldsymbol{C}$ have full row rank, i.e., $\operatorname{rank}(\boldsymbol{A}) = \operatorname{rank}(\boldsymbol{C}) = r \leq m, n$. Given an input ellipsoid $\mathcal{E}_{\boldsymbol{x}}(\boldsymbol{c}_{\boldsymbol{x}}, \boldsymbol{P}_{\boldsymbol{x}})$, the output is an ellipsoid $\mathcal{E}_{\boldsymbol{y}}(\boldsymbol{c}_{\boldsymbol{y}}, \boldsymbol{P}_{\boldsymbol{y}})$ with $\boldsymbol{c}_{\boldsymbol{y}}$ being a point that satisfies $\boldsymbol{A}\boldsymbol{c}_{\boldsymbol{x}} + \boldsymbol{C}\boldsymbol{c}_{\boldsymbol{y}} + \boldsymbol{b} = \boldsymbol{0}$. The generalized propagation formula (Ros et al., 2002)

$$\boldsymbol{P}_{\boldsymbol{y}} = \boldsymbol{C}^\mathsf{T}(\boldsymbol{A}^\mathrm{r})^\mathsf{T}(\boldsymbol{P}_{\boldsymbol{x}} - \boldsymbol{P}_{\boldsymbol{x}}\boldsymbol{N}_A(\boldsymbol{N}_A^\mathsf{T}\boldsymbol{P}_{\boldsymbol{x}}\boldsymbol{N}_A)^\dagger\boldsymbol{N}_A^\mathsf{T}\boldsymbol{P}_{\boldsymbol{x}})\boldsymbol{A}^\mathrm{r}\boldsymbol{C} \tag{9}$$

applies, where $\boldsymbol{N}_A$ is an orthonormal basis for the null space of $\boldsymbol{A}$, and $\boldsymbol{A}^\mathrm{r} = \boldsymbol{A}^\mathsf{T}(\boldsymbol{A}\boldsymbol{A}^\mathsf{T})^{-1}$ is the right pseudo-inverse of $\boldsymbol{A}$. The formula also allows for $\boldsymbol{P}_{\boldsymbol{x}}$ being rank-deficient with $(\cdot)^\dagger$ denoting the Moore-Penrose pseudo-inverse.

3. Ellipsoidal Possibility Distributions

We define an ellipsoidal possibility distribution π in dimension n such that every α-cut

$$\mathcal{C}_\pi^\alpha = \{\boldsymbol{x} \in \mathbb{R}^n \mid \pi_{\boldsymbol{X}}(\boldsymbol{x}) \geq \alpha\} = \mathcal{E}(\boldsymbol{c}_\alpha, \boldsymbol{P}_\alpha) = \{\boldsymbol{x} \in \mathbb{R}^n \mid (\boldsymbol{x} - \boldsymbol{c}_\alpha)^\mathsf{T}\boldsymbol{P}_\alpha(\boldsymbol{x} - \boldsymbol{c}_\alpha) \leq 1\} \tag{10}$$

corresponds to a (hyper)-ellipsoid. Possibility theory requires that for any two possibility levels $0 \leq \alpha_1 \leq \alpha_2 \leq 1$, the ellipsoids $\mathcal{E}_{\alpha_2}$ and $\mathcal{E}_{\alpha_1}$ satisfy the nesting property $\mathcal{E}_{\alpha_2} \subseteq \mathcal{E}_{\alpha_1}$.

This work uses a discrete representation of π consisting of N nested ellipsoids and a residual possibility value $\rho \in [0,1)$. The discrete representation

$$\mathring{\pi} = \left(\{(\mathcal{E}_i, \alpha_i)\}_{i=1}^N,\, \rho\right) \quad \text{with} \quad \rho < \alpha_1 < \ldots < \alpha_N \leq 1 \tag{11}$$

orders the ellipsoids specificity such that $\mathcal{E}_N \subseteq \mathcal{E}_{N-1} \subseteq \ldots \subseteq \mathcal{E}_1$, as illustrated in Figure 1. The possibility value $\pi(\boldsymbol{x})$ for any point $\boldsymbol{x} \in \mathbb{R}^n$ is the highest possibility level where an α-cut contains $\boldsymbol{x}$. If $\boldsymbol{x}$ falls outside the largest ellipsoid $\mathcal{E}_1$, the possibility value evaluates to the residual term ρ. Thus, the possibility function is given by

$$\pi(\boldsymbol{x}) = \max\left(\{\alpha_i \mid \boldsymbol{x} \in \mathcal{E}_i, (\mathcal{E}_i, \alpha_i) \in \mathring{\pi}\} \cup \{\rho\}\right)\ . \tag{12}$$

The residual term ρ is introduced to allow for non-zero possibility values outside the largest ellipsoid $\mathcal{E}_1$, acknowledging that values outside the largest α-cut are not impossible but merely less plausible.

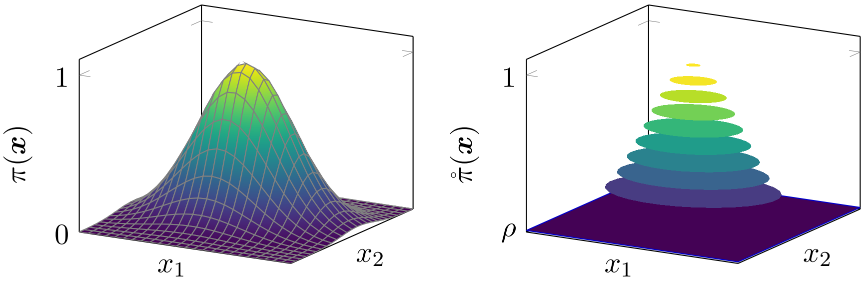

Figure 1. Continuous 2d possibility distribution π (left) and selected α-cuts (right) for the discrete ellipsoidal possibility distribution $\mathring{\pi}$.

3.1. Construction of Ellipsoidal Possibility Distributions

Uncertainty analysis invariably requires, as its first step, an appropriate mathematical model of the information at hand. This section details two such modeling approaches: the construction of ellipsoidal possibility distributions from data and from a given probability density function.

3.1.1. *Construction from Data*

The construction of an ellipsoidal possibility distribution from a dataset $\mathcal{D} = \{\boldsymbol{z}_j\}_{j=1}^{M} \subset \mathbb{R}^n$ requires determining N nested ellipsoids $\{\mathcal{E}_k\}_{k=1}^{N}$ that capture the data's distribution and subsequently assigning possibility values $\{\alpha_k\}_{k=1}^{N}$ that follow some statistical validity criterion. We employ a moment-based approach to determine a concentric and co-oriented structure for the nested ellipsoids $\{\mathcal{E}_k\}_{k=1}^{N}$, as illustrated in Figure 2. The sample mean $\boldsymbol{c} = \frac{1}{M}\sum_{j=1}^{M}\boldsymbol{z}_j$ serves as the common center for all ellipsoids $\mathcal{E}_k(\boldsymbol{c}, \boldsymbol{P}_k)$. The sample covariance matrix $\boldsymbol{\Sigma} = \frac{1}{M}\sum_{j=1}^{M}(\boldsymbol{z}_j - \boldsymbol{c})(\boldsymbol{z}_j - \boldsymbol{c})^{\mathsf{T}}$ determines the shape $\boldsymbol{P}_1 = \boldsymbol{\Sigma}^{-1}$ of the ellipsoids. To establish the outermost ellipsoid $\mathcal{E}_1$, $\boldsymbol{P}_1$ is scaled such that $\mathcal{E}_1(\boldsymbol{c}, \boldsymbol{P}_1)$ strictly encloses the MVEE of $\mathcal{D}$. Subsequent smaller ellipsoids are generated by scaling the shape matrices $\boldsymbol{P}_k = s\boldsymbol{P}_{k-1}$ with a factor $s > 1$, which guarantees nesting. The scaling factor s is determined based on the data dimensionality n and the desired number of ellipsoids N. For instance, achieving a specific geometric progression in the volumes of successive ellipsoids can lead to a reasonable choice for the scaling factor.

The nested ellipsoids are then transformed into a possibility distribution $\mathring{\pi}$ by assigning possibility levels α_k based on the statistical reliability of the data coverage. To account for finite sample sizes, the *reliable membership transform* (Hose, 2022) is employed rather than simple empirical frequency. The level α_k corresponds to the upper confidence bound of the probability that a new sample falls outside the subsequent inner ellipsoid $\mathcal{E}_{k+1}$. Using the reliable possibility distribution estimation, this is calculated with the inverse of the beta cumulative density function

$$\alpha_k = \mathrm{beta}^{-1}(1 - \delta, M_{k+1}^{\mathrm{out}} + 1, M - M_{k+1}^{\mathrm{out}}) \,, \tag{13}$$

where δ defines the confidence level and M_{k+1}^{out} is the number of data points lying outside $\mathcal{E}_{k+1}$. For the innermost ellipsoid, the possibility level is set to $\alpha_N = 1$. Crucially, even if $\mathcal{E}_2$ fully encloses the dataset ($M_2^{\mathrm{out}} = 0$), Equation (13) yields $\alpha_1 > 0$. This ensures a non-zero residual possibility ρ for the unobserved region outside $\mathcal{E}_1$, explicitly acknowledging sampling uncertainty inherent to finite datasets. Finally, redundant levels are pruned to ensure strictly increasing α_k.

Alternatively, the level-defining ellipsoids can be constructed by iteratively removing the outermost data points from $\mathcal{D}$ to get smaller and smaller subsets of data. The sequence begins with the MVEE of the full dataset $\mathcal{D}$. Subsequent inner ellipsoids are generated by computing the MVEE of the subset remaining after removing the boundary points that define the previous iteration. To guarantee strict nesting $\mathcal{E}_k \subset \mathcal{E}_{k-1}$, the bisection-based optimization method from (Calbert et al., 2023) is employed to adjust the ellipsoid parameters. Notably, this same method serves to identify the scaling of $\boldsymbol{P}_{\text{init}}$ required to enclose the MVEE in the moment-based method. Regardless of the geometric derivation, the final distribution is constructed by applying the reliable membership transform to the resulting nested sequence. Additionally, arbitrary distributions can be approximated by a concentric, co-aligned equivalent by computing possibility-weighted averages of the centers and shape matrices.

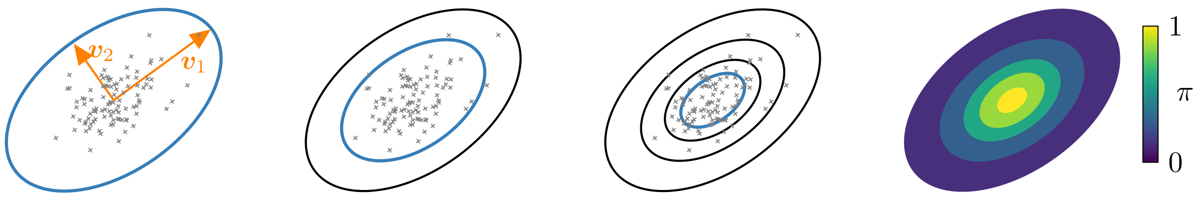

Figure 2. Step-by-step moment-based construction of an ellipsoidal possibility distribution. The sample mean and covariance determine the center and orientation (eigenvectors $\boldsymbol{v}_1, \boldsymbol{v}_2$) of the initial ellipsoid. A sequence of nested ellipsoids is generated by scaling the shape matrix, ensuring a co-aligned structure. The final distribution $\mathring{\pi}$ is obtained by mapping the reliable coverage probability of each ellipsoid to a possibility level α (color scale).

3.1.2. *Construction from Probability Density Functions*

Given an arbitrary probability density function, a consistent possibility distribution can be derived by sampling from the probability density and applying the moment-based inference method described in Section 3.1.1.

Although sampling is applicable to any probability density, an exact analytical construction is possible when the probability density $p(\boldsymbol{x})$ is a multivariate Gaussian distribution $\mathcal{N}(\boldsymbol{\mu}, \boldsymbol{\Sigma})$ with mean $\boldsymbol{\mu}$ and regular covariance matrix $\boldsymbol{\Sigma}$. Because the level sets of a Gaussian distribution are inherently ellipsoidal, they map directly to an ellipsoidal possibility distribution. Following the probability-to-possibility transformation principle (Dubois et al., 2004), this analytical mapping defines the resulting possibility distribution $\pi(\boldsymbol{x})$ as the probability of a density value being lower than or equal to $p(\boldsymbol{x})$.

Consequently, the ellipsoidal level sets are determined by the Mahalanobis distance associated with the specific quantile of the Chi-squared distribution, see (Martin and Williams, 2025). For a possibility level $\alpha \in (\rho, 1]$, the α-cut is then given by

$$\mathcal{C}_\pi^\alpha = \left\{ \boldsymbol{x} \in \mathbb{R}^n \mid (\boldsymbol{x} - \boldsymbol{\mu})^\mathsf{T} \boldsymbol{\Sigma}^{-1} (\boldsymbol{x} - \boldsymbol{\mu}) \leq F_{\chi_n^2}^{-1}(1 - \alpha) \right\} , \tag{14}$$

where $F_{\chi_n^2}^{-1}$ is the inverse cumulative distribution function of the Chi-squared distribution with n degrees of freedom.

3.2. Fusion of Ellipsoidal Possibility Distributions

The combination of multiple sources of information is another central operation in uncertainty quantification. Given two discrete ellipsoidal possibility distributions $\mathring{\pi}_1 = \{(\mathcal{E}_{1,i}, \alpha_{1,i})\}_{i=1}^{N_1}$ and $\mathring{\pi}_2 = \{(\mathcal{E}_{2,j}, \alpha_{2,j})\}_{j=1}^{N_2}$, the objective is to compute a single fused distribution $\mathring{\pi}_{\text{fused}}$ that represents the combined knowledge. A level-wise combination (fusing α-cuts at identical levels) is often infeasible because independently inferred distributions rarely share common levels. Furthermore, interpolating intermediate levels to create a matching level grid implies unjustified precision, which violates the principles of uncertainty quantification.

To address this, we employ a fusion strategy that uses a bidirectional approach to fuse the ellipsoids. First, for every ellipsoid-level $(\mathcal{E}_{1,i}, \alpha_{1,i}) \in \mathring{\pi}_1$, we identify the corresponding ellipsoid-level $(\mathcal{E}_{2,j}, \alpha_{2,j}) \in \mathring{\pi}_2$ with the smallest possibility level $\alpha_{2,j} \geq \alpha_{1,i}$. These two ellipsoids are fused. The process is then repeated from the perspective of $\mathring{\pi}_2$, fusing each $\mathcal{E}_{2,j}$ from $\mathring{\pi}_2$ with the corresponding one in $\mathring{\pi}_1$. Figure 3(a)-(d) visualizes this level-wise pairing and subsequent outer approximation. For a single fusion step between two identified ellipsoids $\mathcal{E}_{1,i}(\boldsymbol{c}_{1,i}, \boldsymbol{P}_{1,i})$ and $\mathcal{E}_{2,j}(\boldsymbol{c}_{2,j}, \boldsymbol{P}_{2,j})$, we seek a tight ellipsoidal outer approximation of their intersection. We utilize the λ-ellipsoid method described in Section 2.2, which provides a parameterized family of ellipsoids $\mathcal{E}_\lambda$ containing the intersection $\mathcal{E}_{1,i} \cap \mathcal{E}_{2,j}$. The shape matrix $\boldsymbol{P}_{\lambda,i,j}$ and center $\boldsymbol{c}_{\lambda,i,j}$ are computed analytically as

$$\boldsymbol{P}_{\lambda,i,j} = \frac{1}{K_{i,j}(\lambda)} \boldsymbol{E}_{\lambda,i,j} \ , \qquad \boldsymbol{c}_{\lambda,i,j} = \boldsymbol{E}_{\lambda,i,j}^{-1} (\lambda \boldsymbol{P}_{1,i} \boldsymbol{c}_{1,i} + (1-\lambda) \boldsymbol{P}_{2,j} \boldsymbol{c}_{2,j}) \tag{15}$$

with

$$\begin{aligned} \boldsymbol{E}_{\lambda,i,j} &= \lambda \boldsymbol{P}_{1,i} + (1-\lambda) \boldsymbol{P}_{2,j} \qquad \text{and} \\ K_{i,j}(\lambda) &= 1 + \boldsymbol{c}_{\lambda,i,j}^\top \boldsymbol{E}_{\lambda,i,j} \boldsymbol{c}_{\lambda,i,j} - \left(\lambda \boldsymbol{c}_{1,i}^\top \boldsymbol{P}_{1,i} \boldsymbol{c}_{1,i} + (1-\lambda) \boldsymbol{c}_{2,j}^\top \boldsymbol{P}_{2,j} \boldsymbol{c}_{2,j} \right) \ . \end{aligned} \tag{16}$$

To maximize information gain, we select the optimal $\lambda^\star$ that minimizes the volume of the resulting λ-ellipsoids. This is equivalent to the optimization problem

$$\lambda_{i,j}^\star = \arg \min_{\lambda \in [0,1]} \left(-\log(\det(\boldsymbol{E}_{\lambda,i,j})) + n \log(K_{i,j}(\lambda)) \right) \ . \tag{17}$$

Alternatively, heuristic choices, such as $\lambda = 0.5$ or weighting based on the trace of the shape matrices, offer computationally cheaper alternatives while remaining reasonable approximations of the optimal solution.

A new possibility value is assigned to the fused ellipsoid. Assuming the information sources are stochastically independent, the independence copula from Equation (6) is employed. This copula ensures consistency and has, by definition, a lifting property: If both sources agree on a region, the possibility of that region increases.

The independent fusion of various levels does not strictly guarantee the fundamental nesting property ($\mathcal{E}_{\text{fused},k} \subseteq \mathcal{E}_{\text{fused},k-1}, k \in \{1, \ldots, N_{\text{fused}}\}$) for the resulting set of ellipsoids. Therefore, we check the inclusion between adjacent levels using the method proposed by (Calbert et al., 2023). If an inner ellipsoid is not fully contained within the outer one, as seen in Figure 3(e), the outer ellipsoid is inflated by scaling its shape matrix such that strict inclusion is satisfied. This ensures that the final output $\mathring{\pi}_{\text{fused}}$ is an ellipsoidal possibility distribution, as demonstrated in Figure 3(f).

Duplicate levels (where $\alpha_{1,i} = \alpha_{2,j}$) are eliminated by retaining only the most specific ellipsoid—the one with the smallest volume—for each unique possibility level.

A key advantage of this approach is the preservation of original α-levels. Furthermore, the method remains applicable to distributions defined by only a few levels or even single intervals.

The proposed framework naturally extends to the fusion of $M > 2$ information sources by generalizing Equation (15) to $\boldsymbol{P}_{\boldsymbol{\lambda}} = \sum_{i=1}^{M} \lambda_i \boldsymbol{P}_i$ with $\boldsymbol{\lambda} \in \mathbb{R}^M$ and $\sum_{i=1}^{M} \lambda_i = 1$. The joint distribution is obtained by fusing at each step M ellipsoids with the independence copula generalizing to $\alpha_{\text{fused}} = 1 - (1-\alpha)^M$, see Equation (6).

While the presented fusion strategy becomes computationally demanding for multiple sources, a synchronized approach—standardizing distributions to a common possibility level discretization and performing simultaneous M-way ellipsoidal fusion—provides a tractable alternative.

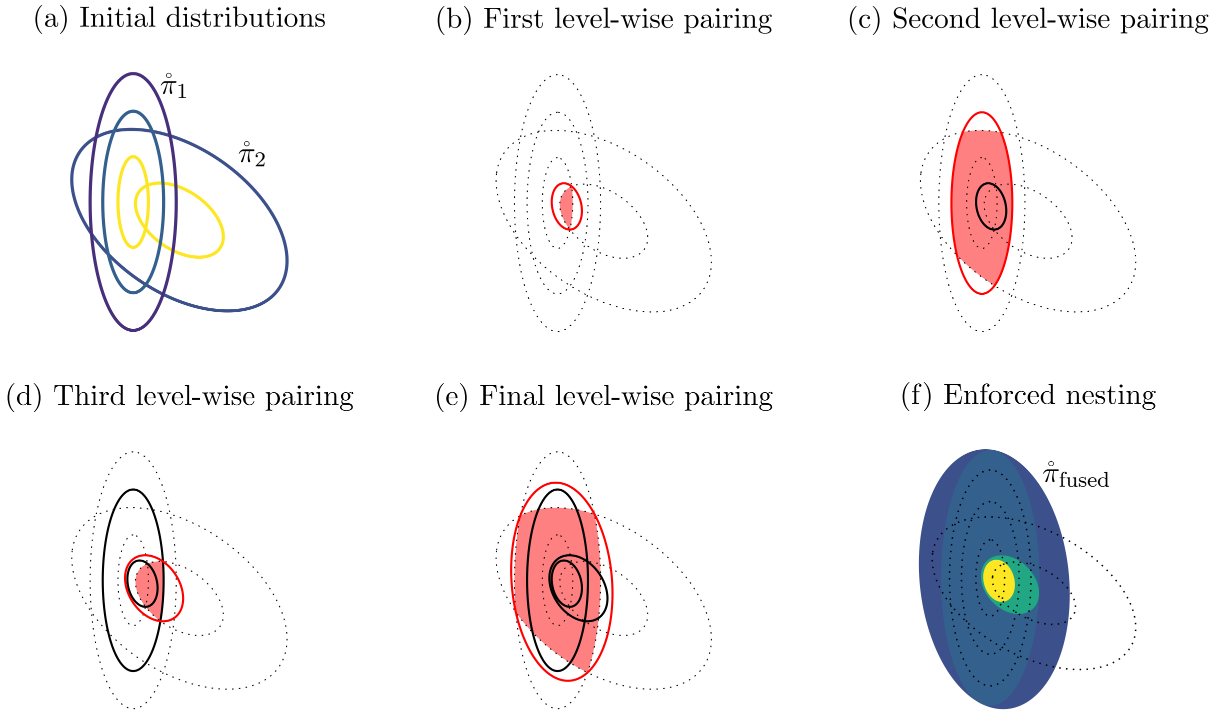

Figure 3. Step-by-step visualization of the fusion procedure for two discrete ellipsoidal possibility distributions. (a) The initial distributions $\mathring{\pi}_1$ and $\mathring{\pi}_2$. (b)-(d) Sequential fusion of corresponding α-cuts to generate new ellipsoids (red). (e) The collection of fused ellipsoids, which may initially violate the nesting property. (f) Expansion of the outer ellipsoids to guarantee nesting, yielding the final valid possibility distribution $\mathring{\pi}_{\text{fused}}$.

3.3. Propagation of Ellipsoidal Possibility Distributions

Given an (ellipsoidal) possibilistic description of uncertainty in state $\boldsymbol{x}$ and a model $\boldsymbol{f}$, uncertainty propagation is concerned with determining the induced possibility distribution of the output $\boldsymbol{y} = \boldsymbol{f}(\boldsymbol{x})$. In the following, a propagation rule for affine mappings is derived, and the general case of nonlinear mappings is discussed.

3.3.1. *Affine Propagation*

Specializing the general implicit relation from Section 2.2 to the explicit affine mapping $\boldsymbol{y} = \boldsymbol{A}\boldsymbol{x} + \boldsymbol{b}$ by setting $\boldsymbol{C} = -\boldsymbol{I}$, we obtain the following propagation rules. Let the input variable $\boldsymbol{x}$ be described by a discrete ellipsoidal possibility distribution $\mathring{\pi}_x = \{(\mathcal{E}_{x,i}, \alpha_i)\}_{i=1}^N$ with $\mathcal{E}_{x,i} = \mathcal{E}(\boldsymbol{c}_{x,i}, \boldsymbol{P}_{x,i})$. Since affine mappings preserve ellipsoidal shapes, each α-cut is propagated individually and retains its possibility level α_i, as illustrated in Figure 4. Hence, the propagated center and the propagated shape matrix are given by

$$\boldsymbol{c}_{y,i} = \boldsymbol{A}\boldsymbol{c}_{x,i} + \boldsymbol{b} \,, \qquad \boldsymbol{P}_{y,i} = \boldsymbol{A}^{-\mathsf{T}}\boldsymbol{P}_{x,i}\,\boldsymbol{A}^{-1} = (\boldsymbol{A}\boldsymbol{P}_{x,i}^{-1}\boldsymbol{A}^{\mathsf{T}})^{-1}, \tag{18}$$

assuming that $\boldsymbol{A}$ is square and invertible. For rank-deficient or non-quadratic $\boldsymbol{A}$, $\boldsymbol{C}$ or positive semi-definite $\boldsymbol{P}_{x,i}$, the generalized propagation rule in Equation (9) is applied, yielding a possibly degenerate output ellipsoid.

Because affine mappings preserve convexity and set inclusion, the nesting property $\mathcal{E}_{y,N} \subseteq \ldots \subseteq \mathcal{E}_{y,1}$ is retained. The propagated stack $\mathring{\pi}_y = \{(\mathcal{E}_{y,i}, \alpha_i)\}_{i=1}^N$ thus constitutes a valid ellipsoidal possibility distribution without loss of information.

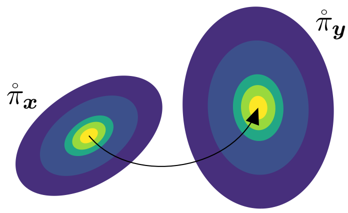

Figure 4. Affine propagation of a discrete ellipsoidal possibility distribution $\mathring{\pi}_{\boldsymbol{x}}$ resulting in the output distribution $\mathring{\pi}_{\boldsymbol{y}}$.

3.3.2. *Nonlinear Propagation*

For nonlinear mappings $\boldsymbol{f}$, the level sets induced by the extension principle are generally non-ellipsoidal and cannot be propagated analytically.

One approach is to sample from each $\mathcal{E}_{x,i}$, propagate the samples through $\boldsymbol{f}$, and reconstruct an ellipsoidal distribution using the data-based construction proposed in Section 3.1. Another approach is to linearize $\boldsymbol{f}$ about the center of each ellipsoid $\mathcal{E}_{x,i}$ and use affine propagation to obtain the propagated ellipsoids. Linearization errors can be enclosed by ellipsoidal outer bounds, as demonstrated for Kalman filters in (Noack et al., 2010). Incorporating these bounds via Minkowski-sum approximations ensures the resulting output distribution remains a conservative outer approximation.

3.4. Marginal and Joint Ellipsoidal Possibility Distributions

The final fundamental operation necessary for a complete uncertainty calculus is the ability to derive marginal distributions from joint distributions and to construct joint distributions from marginals. The proposed framework handles both operations geometrically through propagation and fusion.

3.4.1. *Marginalization*

Given a joint discrete ellipsoidal possibility distribution $\mathring{\pi}_{\boldsymbol{x}} = \{(\mathcal{E}_{\boldsymbol{x},i}, \alpha_i)\}_{i=1}^{N}$ defined on $\mathbb{R}^n$, the marginal distribution for a subspace of variables is obtained by projecting each ellipsoidal α-cut onto that subspace. In possibility theory, marginalization corresponds to the supremum operator, which, for convex sets, is equivalent to geometric projection. For an ellipsoid $\mathcal{E}_{\boldsymbol{x}}(\boldsymbol{c}_{\boldsymbol{x}}, \boldsymbol{P}_{\boldsymbol{x}})$, the projection onto a subspace is defined by a diagonal transformation matrix $\boldsymbol{A}$, which contains ones on the diagonal for the axes onto which the ellipsoid is projected and zeros elsewhere. In the context of Equation (9), this is equivalent to an affine propagation with singular matrix $\boldsymbol{A}$ and $\boldsymbol{b} = \boldsymbol{0}$, yielding a degenerate marginal ellipsoid $\mathcal{E}_{\boldsymbol{y}}(\boldsymbol{c}_{\boldsymbol{y}}, \boldsymbol{P}_{\boldsymbol{y}})$ with $\boldsymbol{c}_{\boldsymbol{y}} = \boldsymbol{A}\boldsymbol{c}_{\boldsymbol{x}}$ and $\boldsymbol{P}_{\boldsymbol{y}} = \boldsymbol{A}^{\mathsf{T}}(\boldsymbol{A}\boldsymbol{P}_{\boldsymbol{x}}^{\dagger}\boldsymbol{A}^{\mathsf{T}})^{\dagger}\boldsymbol{A}$. This operation is applied element-wise to the sequence of nested ellipsoids. Since projection is a linear mapping, convexity and nesting of the ellipsoidal α-cuts are preserved, ensuring that the resulting collection $\mathring{\pi}_{\boldsymbol{y}} = \{\mathcal{E}_{\boldsymbol{y},i}, \alpha_i\}_{i=1}^{N}$ constitutes a marginal ellipsoidal possibility distribution.

3.4.2. *Joint Distributions from Marginals*

Constructing a joint distribution from a set of marginal distributions $\{\mathring{\pi}_1, \ldots, \mathring{\pi}_d\}$ involves approximating the Cartesian product of the marginal α-cuts. Geometrically, the Cartesian product of d marginal ellipsoids (or intervals) forms a hyperrectangle in the joint space $\mathbb{R}^n$, which is not an ellipsoid. To maintain the ellipsoidal representation, we construct a tight ellipsoidal outer approximation of this hyperrectangle. Figure 5 illustrates this bounding process for two marginals, showing how the nested intervals define hyperrectangles enclosed by optimal ellipses.

We achieve this by treating each marginal α-cut as a degenerate ellipsoid (a cylinder) in the full joint space, unbounded in all dimensions orthogonal to the jth subspace. A closed-form solution exists for the fusion of independent marginals defined on complementary subspaces (e.g., combining $\boldsymbol{x}_1$ and $\boldsymbol{x}_2$ where $\boldsymbol{x} = [\boldsymbol{x}_1^{\mathsf{T}}, \boldsymbol{x}_2^{\mathsf{T}}]^{\mathsf{T}}$). If marginals are not only defined on complementary subspaces, but also intersect, the intersecting subspace marginals can be fused first with the fusion procedure described in Section 3.2. Following (Ros et al., 2002), if the rank sum of the shape matrices equals the full dimension $(\mathrm{rank}(\boldsymbol{P}_1) + \mathrm{rank}(\boldsymbol{P}_2) = n)$, the parameters

$$\boldsymbol{c}_{\text{joint}} = (\boldsymbol{P}_1^2 + \boldsymbol{P}_2^2)^{-1}(\boldsymbol{P}_1^2\boldsymbol{c}_1 + \boldsymbol{P}_2^2\boldsymbol{c}_2) \qquad \text{and} \qquad \boldsymbol{P}_{\text{joint}} = \frac{p}{n}\boldsymbol{P}_1 + \frac{n-p}{n}\boldsymbol{P}_2 \tag{19}$$

of the optimal joint α-cut $\mathcal{C}_{\text{joint}}^{\alpha}$ are given analytically, where $p = \mathrm{rank}(\boldsymbol{P}_1)$. Note that the resulting ellipsoid is in fact the MVEE of the Cartesian product of the marginal ellipsoids defined in a higher dimensional space. Repeating this process for all α-levels produces a nested sequence that forms the joint ellipsoidal possibility distribution $\mathring{\pi}_{\text{joint}}$. The effect of this adjustment is visible on the right-hand side of Figure 5, where the copula application lifts the second possibility level. Depending on the assumed dependency structure, the possibility levels may need to be adjusted using an appropriate copula like the independence copula in Equation (6).

4. Case Study: State Estimation of an Omnidirectional Robot

To demonstrate the functionality of the proposed framework, we apply it to a state estimation problem for a wheeled mobile robot. We utilize a recursive possibilistic filter (Hose and Hanss,

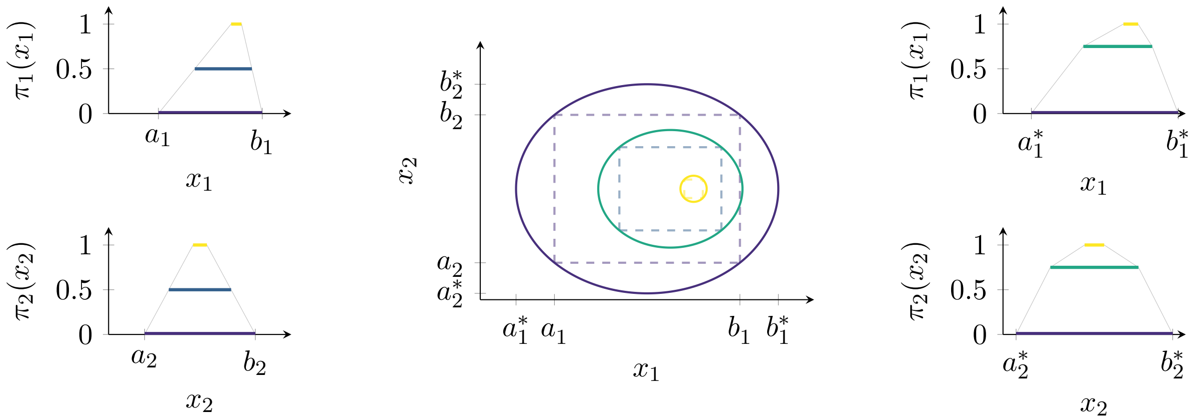

Figure 5. Illustration of constructing a joint ellipsoidal possibility distribution from two marginal triangular distributions and vice versa. The α-cuts of the marginals on the left-hand side form nested intervals, which define nested hyperrectangles in the joint space, enclosed by the tightest possible ellipsoids. The independence copula is applied, when joining the marginals, resulting in the lifted middle level on the right-hand side.

2021) built upon the previously derived ellipsoidal possibility distributions and their calculus. The considered robot is an omnidirectional platform, see Figure 6 (left) and (Ebel, 2021) for details, whose kinematics is described by the discrete-time linear system

$$\boldsymbol{x}_k = \boldsymbol{x}_{k-1} + \delta_t \boldsymbol{u}_{k-1} + \boldsymbol{v}_{k-1}, \tag{20}$$

where, at time step $k \in \mathbb{N}_0$, the state vector $\boldsymbol{x}_k = [x_k \ y_k \ \theta_k]^\mathsf{T} \in \mathcal{X} \subseteq \mathbb{R}^3$ represents the robot pose, $\boldsymbol{u}_k = [v_{x,k} \ v_{y,k} \ \omega_k]^\mathsf{T} \in \mathcal{U} \subset \mathbb{R}^3$ denotes the applied control input, $\boldsymbol{v}_k$ is the process noise, and $\delta_t > 0\,\mathrm{s}$ is the sampling time.

Full-state measurements are obtained in the academic hardware testbed using a motion capture system. Since the motion capture system provides highly accurate pose estimates, the recorded data is treated as ground truth $\boldsymbol{x}_k$. Artificial measurement noise $\boldsymbol{w}_k$ is then added synthetically, yielding measurements $\boldsymbol{y}_k$ with known, controllable noise characteristics while retaining access to the true states for validation. The resulting observation model is

$$\boldsymbol{y}_k = \boldsymbol{x}_k + \boldsymbol{w}_k. \tag{21}$$

The measurement noise is modeled as a zero-mean multivariate normal distribution with covariance matrix $\boldsymbol{\Sigma}_w = \mathrm{diag}([(5\,\mathrm{mm})^2 \ (5\,\mathrm{mm})^2 \ (5^\circ)^2])$. Due to hardware imperfections and manufacturing inaccuracies, the process noise is accounted for by adding constant offsets $\varepsilon_{xy} = 10\,\mathrm{mm}$ and $\varepsilon_\theta = 1^\circ$ to the semi-axes for position and orientation of the propagated ellipsoids, respectively. In other words, since the ellipsoids are axis-aligned, with shape matrix $\boldsymbol{P} = \mathrm{diag}([p_x, \, p_y, \, p_\theta])$, each diagonal entry is updated as

$$p_i' = \left(\frac{1}{\sqrt{p_i}} + \varepsilon_i \right)^{-2}, \tag{22}$$

where $\varepsilon_x = \varepsilon_y = \varepsilon_{xy}$ and ε_θ as defined above.

The task of state estimation is demonstrated using a dataset collected from the real-world robot. An open-loop input sequence is applied, nominally driving the robot along a lemniscate-shaped trajectory. In total, $N_t = 159$ control commands are sent to the robot at a sampling time of $\delta_t = 0.2\,\mathrm{s}$ using a zero-order hold. The corresponding state measurements are recorded at the same sampling rate. The robot is manually placed at the initial pose $\boldsymbol{x}_0 = [0\,\mathrm{m}\ 0\,\mathrm{m}\ 30.96°]^\mathsf{T}$. Placement inaccuracies are accounted for by an initial uniform possibility distribution $\pi_{\tilde{X}_0}$ supported on the set $\mathcal{X}_0 = ([-0.5, 0.5]\mathrm{m})^2 \times [-45, 45]°$. The measurements are plotted in the right-hand part of Figure 6, showing the temporal evolution of the robot's pose as recorded by the motion capture system.

The initialized recursive filter follows the standard prediction-inversion-update structure. A brief outline of the filter is given in the following and illustrated schematically in Figure 7 (left) for a selected number of time instants. See, e.g., (Hose and Hanss, 2021) for further details.

In the *prediction step*, the information about the previous state $\boldsymbol{x}_{k-1}$ is propagated through the system dynamics from Equation (20) using the affine propagation of ellipsoidal possibility distributions, see Section 3.3.1. This yields a predicted ellipsoidal possibility distribution $\mathring{\pi}_{\mathrm{p},k}$ of the successor state $\boldsymbol{x}_k$, taking into account the uncertainty in the previous state as well as the process noise. In the subsequent *inversion step*, the current measurement $\boldsymbol{y}_k$ is used to construct a second possibility distribution $\mathring{\pi}_{\mathrm{i},k}$ describing $\boldsymbol{x}_k$. This is achieved by applying a probability-to-possibility transformation to the known noise distribution, see Section 3.1.2. Finally, in the *update step*, the two distributions obtained from the prediction and inversion steps are fused to $\mathring{\pi}_{\mathrm{fused},k}$ using the fusion rule for ellipsoidal possibility distributions, see Section 3.2. This recursive procedure is repeated for each of the N_t time steps, resulting in a sequence of ellipsoidal possibility distributions that describe the temporal evolution of the robot's state estimate.

Figure 7 illustrates the results of the state-estimation process. The left plot shows the ellipsoidal possibility distributions at selected time instances, visualized as nested ellipses corresponding to different possibility levels. The right-hand plot in Figure 7 shows the empirical coverage probabilities

$$\hat{p}(\alpha) = \frac{1}{N_t + 1} \left| k \in \mathbb{Z}_{0:N_t} : \boldsymbol{x}_k \in \mathcal{C}^{\alpha}_{\mathring{\pi}_{\mathrm{fused},k}} \right| , \tag{23}$$

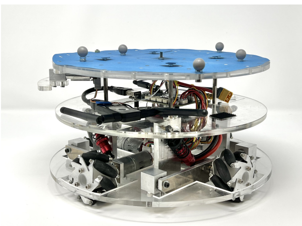

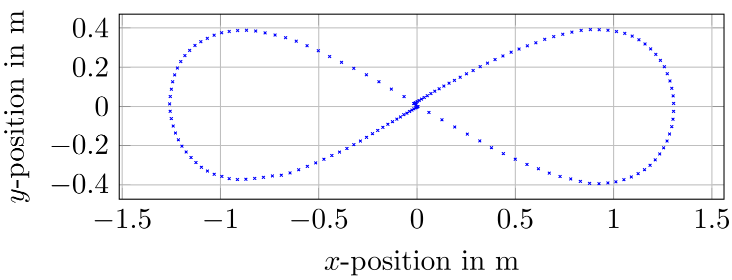

Figure 6. Experimental setup. Left: The HERA omnidirectional robot platform. Right: Recorded state measurements from the motion capture system.

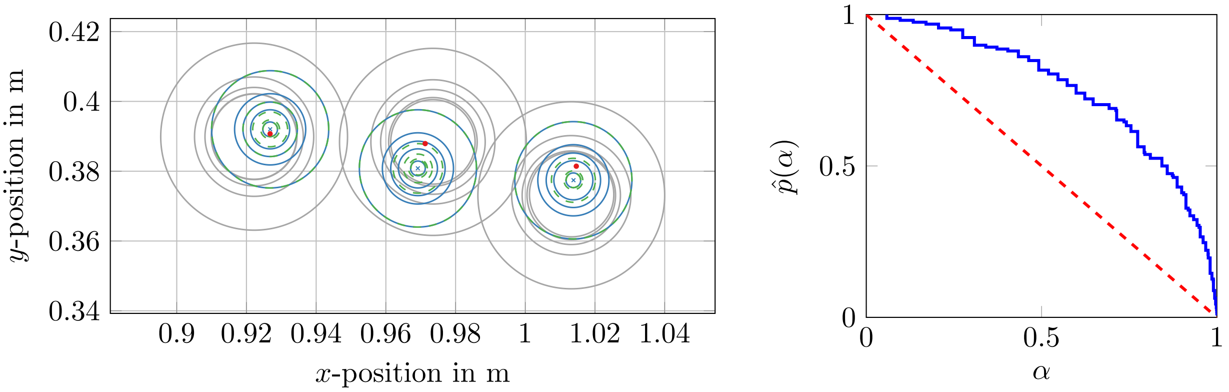

Figure 7. Results of the filtering procedure. Left: Projection onto the x-y plane for timesteps 32–34. Gray ellipses show the predicted distributions, blue ellipses the measurement distributions, and green ellipses the fused distributions. Red dots indicate the true states, blue crosses the measurements. Right: Empirical coverage curve, validating the performance of the filter.

that is, the fraction of time steps for which the true state $\boldsymbol{x}_k$ lies within the α-cut of the estimated distribution. A coverage curve above the diagonal indicates the filter's validity, as prescribed by Equation (4). For more insight into these curves, see (Wimbush et al., 2022).

The results show that the filter successfully tracks the true state with the prescribed confidence. However, the comparatively high process noise causes the fused estimate to closely follow the measurement distribution, which is more precise than the predicted state. As a result, the filter behaves similarly to a static measurement-only estimator that ignores the system dynamics. This also explains why the projected ellipses of the estimated states are nearly circular, reflecting the isotropic measurement noise.

5. Conclusion and Future Work

This paper presents a novel framework for possibilistic uncertainty modeling based on hyperellipsoids. Leveraging results of ellipsoidal calculus, polymorphic, i.e. aleatory and epistemic, uncertainty is rigorously represented, fused, and propagated using nested ellipsoidal sets. The ellipsoidal approach offers a distinct advantage over common grid-based or sampling methods by providing analytical solutions for linear transformations and preserving correlation information typically lost in axis-aligned interval representations.

The core contribution consists of strategies for the construction, combination, and propagation of arbitrary-dimensional ellipsoidal possibility distributions. Inference methods are introduced to generate ellipsoidal possibilistic distributions from raw data, and the concept of a convex combination of ellipsoidal sets is extended to the fusion of ellipsoidal possibility distributions. Moreover, the marginalization to lower dimensions is detailed and the construction of joint distributions from marginals, framed as a degenerate ellipsoid fusion task, is presented. Furthermore, the framework provides exact analytical propagation for affine functions. The efficacy of this calculus is validated through a linear dynamic state estimation problem, for which an ellipsoidal possibilistic filter successfully tracks the system state within trustworthy confidence regions. Owing to the conservative nature of possibility theory and the reliance on outer approximations, the results remain rather conservative and face limitations regarding over-approximation in repeated fusion operations.

Future work is to optimize the trade-off between computational efficiency and the tightness of uncertainty bounds. Optimization-based intersection methods, such as semi-definite programming, are to be investigated as replacements for the presented heuristic λ-ellipsoid fusion approach, as well as developing explicit solutions for regularly occuring special cases. Additionally, strategies for conflict detection and introducing more flexible sampling-based methods to handle nonlinearities are to be explored.

Acknowledgements

The authors gratefully acknowledge the support provided by the German Research Foundation (DFG) in the framework of the research projects no. 514188140 (HA2798/16-1) and no. 433183605 (EB195/32-2). Julian Behrend thanks the Claussen-Simon-Foundation and Kyb Alumni e.V. for funding his conference participation.

References

Calbert, J., L. N. Egidio, and R. M. Jungers: 2023, 'An efficient method to verify the inclusion of ellipsoids'. *IFAC-PapersOnLine* **56**(2), 1958–1963.

Dubois, D., L. Foulloy, G. Mauris, and H. Prade: 2004, 'Probability-possibility transformations, triangular fuzzy sets, and probabilistic inequalities'. *Reliable Computing* **10**(4), 273–297.

Ebel, H.: 2021, *Distributed Control and Organization of Communicating Mobile Robots: Design, Simulation, and Experimentation*, Doctoral thesis: Schriften aus dem Institut für Technische und Numerische Mechanik der Universität Stuttgart, Vol. 69. Düren: Shaker Verlag.

Ferrero, A., H. V. Jetti, and S. Salicone: 2021, 'The possibilistic Kalman filter: Definition and comparison with the available methods'. *IEEE Transactions on Instrumentation and Measurement* **70**, 1–11.

Hose, D.: 2022, *Possibilistic Reasoning with Imprecise Probabilities: Statistical Inference and Dynamic Filtering*, Doctoral thesis: Schriften aus dem Institut für Technische und Numerische Mechanik der Universität Stuttgart, Vol. 74. Düren: Shaker Verlag.

Hose, D. and M. Hanss: 2021, 'A recursive formulation of possibilistic filters'. In: *Proceedings of the 12th International Symposium on Imprecise Probability: Theories and Applications*, Vol. 147 of *Proceedings of Machine Learning Research*. pp. 180–190.

Kreinovich, V., J. Beck, and H. T. Nguyen: 2007, 'Ellipsoids and ellipsoid-shaped fuzzy sets as natural multi-variate generalization of intervals and fuzzy numbers: How to elicit them from users, and how to use them in data processing'. *Information Sciences* **177**(2), 388–407.

Könecke, T., J. Schneider, and M. Hanss: 2025, 'Sampling-based possibility theory for engineering analysis under uncertainty: inference, prediction and optimization'. In: *Proceedings of the 35th European Safety and Reliability Conference (ESREL2025) and the 33rd Society for Risk Analysis Europe Conference (SRA-E 2025)*. Stavanger, Norway.

Martin, R.: 2025, 'A new Monte Carlo method for valid prior-free possibilistic statistical inference'. *arXiv preprint arXiv:2501.10585*.

Martin, R. and J. P. Williams: 2025, 'Asymptotic efficiency of inferential models and a possibilistic Bernstein–von Mises theorem'. *International Journal of Approximate Reasoning* **180**, 109389.

Matía, F., V. Jiménez, B. P. Alvarado, and R. Haber: 2021, 'The fuzzy Kalman filter: Improving its implementation by reformulating uncertainty representation'. *Fuzzy Sets and Systems* **402**, 78–104.

Moshtagh, N.: 2005, 'Minimum volume enclosing ellipsoid'. *Convex Optimization* **111**, 112.

Mäck, M. and M. Hanss: 2021, 'An advanced sampling technique for possibilistic uncertainty propagation'. *Mechanical Systems and Signal Processing* **147**, 107064.

Noack, B., V. Klumpp, N. Petkov, and U. D. Hanebeck: 2010, 'Bounding linearization errors with sets of densities in approximate Kalman filtering'. In: *Proceedings of the 13th International Conference on Information Fusion*. Edinburgh, UK, pp. 1–8.

Ros, L., A. Sabater, and F. Thomas: 2002, 'An ellipsoidal calculus based on propagation and fusion'. *IEEE Transactions on Systems, Man and Cybernetics, Part B (Cybernetics)* **32**(4), 430–442.

Wimbush, A., N. Gray, and S. Ferson: 2022, 'Singhing with confidence: Visualising the performance of confidence procedures'. *Journal of Statistical Computation and Simulation* **92**(13), 2686–2702.

Zadeh, L. A.: 1975, 'The concept of a linguistic variable and its application to approximate reasoning'. *Information Sciences* **8**(3), 199–249.